XLI CILAMCE
XLI Ibero-Latin American Congress on Computational Methods in Engineering
16-19 November, 2020 FOZ DO IGUAÇU PARANÁ - BRAZIL

Nonlinear finite element modeling of the impact of spherical and sharp brittle particles against a flat surface

S.G.A Araújo[1], T. Doca[2]

[1]*Dept. of Mechanical Engineering, University of Brasilia - UnB*
Darcy Ribeiro, 70910-900, Brasília-DF, Brazil
1 Araujo.samuel@aluno.unb.br
2 Doca@unb.com.br

Abstract. An impact is defined as a sudden transfer of energy between solids, which often leads to forces of high magnitude and subsequent damage. Moreover, the repetitive impact of brittle particles on protective surfaces, enables a failure mechanism known as erosive wear. In this work, a finite element model of the impact of brittle particles is presented. Two geometries are studied: a sphere and a polygon with sharp edges. Firstly, the proposed model is validated, in a linear setting, using the classical Hertz's theory. In a second setting, the particles are regarded as sedimentary rocks while the flat counterpart is defined as a thick layer of steel coated with protective materials. Further analysis, including nonlinear phenomena such as frictional contact, finite inelastic strains, damage and fracture and provided alongside with a discussion on the failure mechanisms observed. Result show the influence of the particle's shape weight and speed on the failure of the counterpart.

Keywords: Nonlinear Analysis, Finite Element, Impact Mechanics, Brittle materials, Coatings.

1 Introduction

The presence of mechanical contact can be observed in almost all manufacturing processes, natural phenomena and daily activities, being a prerequisite for stress/deformation and movement to occur (Doca,2010). The contact between two bodies creates a highly non-linear problem. This is due to the dissipated energy associated mostly with the frictional forces and also because the contact area has a non-linear evolution. In fact, a linear hypothesis is valid under special circumstances and usually involves small deformations and small displacements. Classical analytical solutions are the Hertz formulae (Hertz,1882) and the Cattaneo-Mindlin solution (Cattaneo,1938; Mindlin,1949). However, with the evolution of technology and computational mechanics, a several numerical formulations that address nonlinear contact are available.

A part of the mechanics that studies the collision between two bodies is called impact and is characterized by the production of contact forces in relation to the variations that are carried out over a very short period of time. Therefore, the impact is a phenomenon that involves deformation, material recovery and the dissipation of energy due to friction, heat and sound. Moreover, major changes in the impact process can be caused by minute variations in it's initial setup, dynamical behavior or boundary conditions. For this reason, it is important to analyze and evaluate the results generated from the impact calculations (Merian,2009). The high-speed impact is of interest to many different fields and has been the subject of much research, especially over the past 50 years. During this period, the methods used to analyze the impact changed dramatically, as did the disciplines interested in these analyzes. Researchers are still trying to get a clear picture of the impact behavior (Kiran,2004). Large variations in the impact process are caused by small variations in the impact conditions. For this reason, it is important to analyze and evaluate the results generated from the impact calculations.

Johnson and Cook proposed a material model suitable for materials subjected to large strains, high strain rates and high temperatures. The model was intended primarily for numerical computations (Johnson,1983). The variables used in the model are also available in most commercial finite element codes and it is therefore easy to implement. The Johnson-Cook material model takes the form of a product of dependencies. The material behavior

in function of the multiplicative effects of the strain, strain rate e temperature (Liang,1999). Nowadays, several types of constitutive models for materials are being developed and optimized constantly, together with an increasing need for numerical simulations. Especially for materials under load conditions with large deformations, high strain rates and high pressures (LHH)(Wang,2018). Another model currently used is Concrete Damage Plasticity (CDP), as it is a model idealized by Lubliner (Lubliner,1989) and modified by Lee and Fenves (Lee,1998) based on plasticity and damage mechanics to compute the loss of material stiffness. This model was developed for concrete although, according to SIMULIA (Simulia,2012), it is also valid for other material with almost fragile behavior.

In this work, simulations were carried-out to analyze the impact behavior of two different contact configurations: a sphere-to-flat and sharp edge-to-flat. The particles are regarded as a brittle material whereas the flat counterpart is modeled. The objective of this work is to evaluate the effect of the particle's initial velocity on the equivalent stress distribution.

1.1 Johnson-Cook constitutive model

The Johnson-Cook constitutive model (Johnson,1985) has been selected for this study.

$$\sigma = [\,\mathrm{A} + \mathrm{B}\varepsilon^{n}]\,\left[1 + C\ ln\left(\frac{\dot{\varepsilon}_{eq}}{\dot{\varepsilon}_{0}}\right)\right]\left[1 - \left(\frac{T - T_r}{T_m - T_r}\right)^{m}\right] \tag{1}$$

This model describes the equivalent stress, σ, using three terms, eq (1). The first term is a function of the initial yield stress, A, the plastic resistance, B, the plastic strain, ε, and the hardening index n. The second term includes the effect of the strain rate sensitive, C, the equivalent plastic strain rate $\dot{\varepsilon}_{eq}$ and the reference plastic strain rate $\dot{\varepsilon}_0$. The third term introduces the softening behavior as a function of the body's temperature, T , the melting temperature T_m, the reference temperature T_r and the softening coefficient, m. The third term has not been considered in this study.

1.2 Concrete Damage plastic (CDP) model

In the CDP model, concrete and other materials are seen as cohesive materials with friction, and an eventual loss of stiffness (damage) can be related to a loss of cohesion. The two main forms of damage in this model are cracks due to traction and crushing due to compression, as you can see in figure 1, which separately represents the behavior of the material in traction and uniaxial compression, considering that the responses to these two types of shipments are quite distinct. The CDP model obeys classical theory of plasticity with the following assumptions (Abaqus,2015):

- Additive strain rate decomposition, eq.(2):

$$\dot{\varepsilon} = \dot{\varepsilon}^{e} + \dot{\varepsilon}^{p},. \tag{2}$$

Where $\dot{\varepsilon}^{e}$ is elastic strain rate and $\dot{\varepsilon}^{p}$ is plastic strain rate.

- Scalar damage factor d entering the elasticity stress-strain relation, eq. (3):

$$\sigma = (1 - d)D_0^{el}\colon(\varepsilon - \varepsilon^{p}), \tag{3}$$

Where D_0^{el} is the initial stiffness of the material (undamaged); ε is the total strain; ε^{p} is the plastic strain. Moreover, a yield function $F(\bar{\sigma}, \tilde{\varepsilon}^{P})$ must be attained such that the Kuhn-Tucker condition $\dot{\lambda}\mathrm{F} = 0; \dot{\lambda} \geq 0; \mathrm{F} \leq 0$ is fulfilled alongside with a non-associated potential flow rule eq. (4):

$$\dot{\varepsilon}^{p} = \lambda\frac{\partial \mathrm{G}(\bar{\sigma})}{\partial \bar{\sigma}} \tag{4}$$

Where $\bar{\sigma}$ is the effective stress.

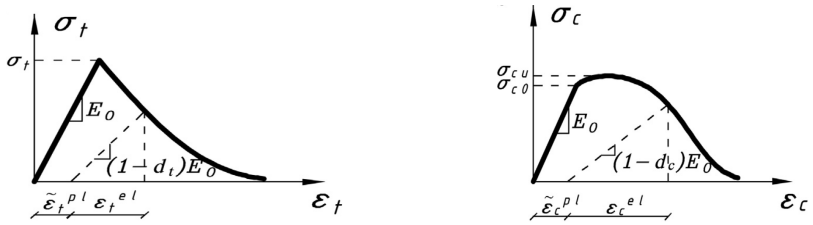

Figure 1. Uniaxial stress-strain curves to illustrate the damage: (a) For tension; (b) For compression

2 Methodology

The analyzed phenomenon is an impact of a brittler materials impacting on a metallic flat counterpart. The repetitive impact of these breaks on the surface allows for a failure mechanism know as erosive wear.

2.1 Modeling and discretization

Two types of brittle material geometry spherical and sharp, impact on a metallic flat counterpart. As it is possible to observe as geometries in figure 2.

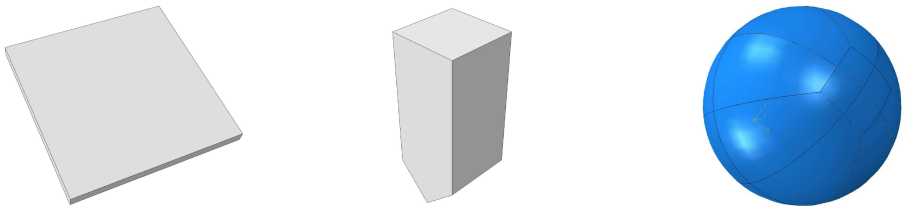

Figure 2. Analyzed geometries: (a) Squared flat counterpart: 100 mm wide and 6.35 mm thick; (b) Sharp indenter: 10 mm wide square section, 26 mm of length and a 45° centered sharp corner; (c) Spherical indenter: 7.5 mm radius

As shown in figure 2, characteristic sizes of small rocks were used and for the metal flat counterpart, only one section was used in order to decrease the total analysis time and the dimensions of the geometries.

The boundary conditions adopted for the spherical and sharp projectiles were restricted to lateral displacement and rotation in the three directions. For the metallic plate, sections were created at the ends and in the configuration of these section restrictions were applied in the three directions.

The loading condition for the projectiles was associated with a speed of 20, 40 and 60 m/s impacting at an angle of 90^{o} (between the velocity vector and the plate surface).

The sensitivity analysis of the mesh was performed on the size of the elements and the type of integration. Call the computational distributions of costs and stresses supported, the first included components were adopted and reduced integration geometries of the target material. The geometry elements related to the target material are of the C3D8R type: 3D stress family, linear order, 8-node hexahedron, with reduced integration, first order and maximum degradation (element is eliminated from the analysis when the total damage is maximum, equal to 1). For the target material, the most a refined mesh was considered in the central impact region, maintaining or controlling the elements adopted in the approximate size of element of 0.2 mm, while for the other regions considered to be of approximately 0.8 mm in size. For the discretization of the projectile, elements with an average size of 0.5 mm were used for the contact zone while the remaining size 0.8 mm elements were employed the remaining parts.

In order to carry out a more in-depth analysis, including the influence of weight variation, particle speed on the flat counterpart failure, a subroutine has been developed.

2.2 Materials

To validate the impact simulation between the projectile and the flat counterpart, Hertz equations were used. Therefore, the type of material applied in the three geometries was the same, aluminum. For the analysis of the nonlinear behavior of the impact generated between two solids, the properties of the concrete in the projectile and the properties of the steel in the flat counterpart were used. The standard properties of steel and aluminum are shown in table 1.

Table 1. Aluminum and AISI 1020 steel properties

Material	Density [kg/m³]	Modulus of elasticity [GPa]	Poisson coefficient
Steel	7830	200	0.30
Aluminum	2700	70	0.35

To obtain a modeling pertinent to the behavior of the steel the formulation of Johnson-Cook was used. The properties of the material used in the analysis are listed in table 1 and the parameters of plasticity model used are A = 333 MPa, B = 737 MPa, n = 0.15 and m=1.46, T_m = 1793 K, T_r = 298, c =0.008 and $\dot{\varepsilon} = 1s^{-1}$(Jasper,2002). The criterion of damage used was the initial criterion and damage evolution law for ductile materials, the damage parameters used were $d_1 = 0.05$, $d_2 = 3.44$; $d_3 = 2.12$; $d_4 = 0.002$ and $d_5 = 0.61$ (Johnson,1985).

A modeling pertinent to the concrete behavior, the CDP model and its respective material properties were used. In addition to the data obtained from the stress strain curves and the properties of table 2, the following plasticity parameters were considered: dilatation angle = 35°, eccentricity = 0.1, relationship between the compressive strength of biaxial and uniaxial concrete = 1.12 and stress factor shape = 0.67. (Mojtaba,2017).

Table 2. Standard concrete properties (Mojtaba,2017)

Compressive stress (MPa)	Inelastic strain (%)	Tensile stress (MPa)	Inelastic strain (%)
9.211	0	3.50	0
12.277	0.0001	3.15	2.24E-005
15.224	0.0002	2.45	0.000269
18.027	0.0003	1.75	0.000448
20.663	0.0004	1.05	0.000628
23.112	0.0005	0.35	0.000807

3 Results and discussions

Figure 3 shows the mesh employed for the discretization of each solid. These problems were analyzed with a finite mesh of finer elements in the story areas to increase the accuracy of the results.

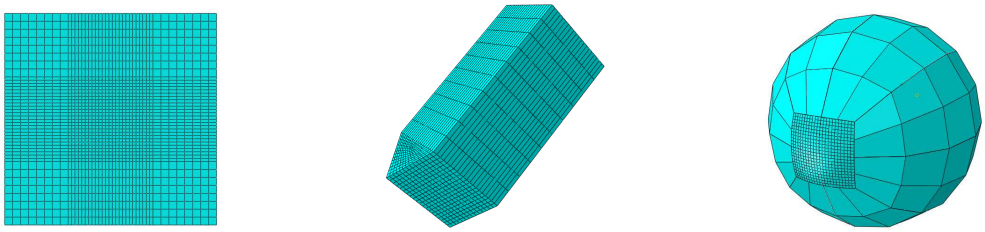

(a) (b) (c)

Figure 3. (a) Flat counterpart; (b) Sharp indenter; (c) Spherical indenter

The data were evaluated in the time interval from 0 seconds to 2 milliseconds. An indentation distance of 0.1 µm was obtained for the first point, the second and third point the indentation distance was 1µm. A comparison between the numerical simulation and the analytical results provided by Hertz's formulae for the indentation depth and the normal stress are giving in table 3. Similar results were obtained for all three velocities which validates this setup for the inelastic analysis.

Table 3: Comparison between numerical simulation and the analytical results for the sphere-to-flat configuration at different impact velocities.

	Numerical Simulation		Analytical results		Relative error	
Velocity (m/s)	*d (µm)*	*Stress (MPa)*	*d (µm)*	Stress (MPa)	*d (%)*	Stress (%)
2.5	0.13	108.90	0.15	109.50	13.33	0.54
5.0	1.43	346.20	1.50	346.29	4.66	0.02
7.5	1.50	352.70	1.50	346.29	0	1.85

The graph in figure 4 shows the simulations of the impact of deformable solids at the velocities of 20 m/s ,40 m/s and 60m/s, with the projectile having concrete properties and the flat counterpart having steel properties.

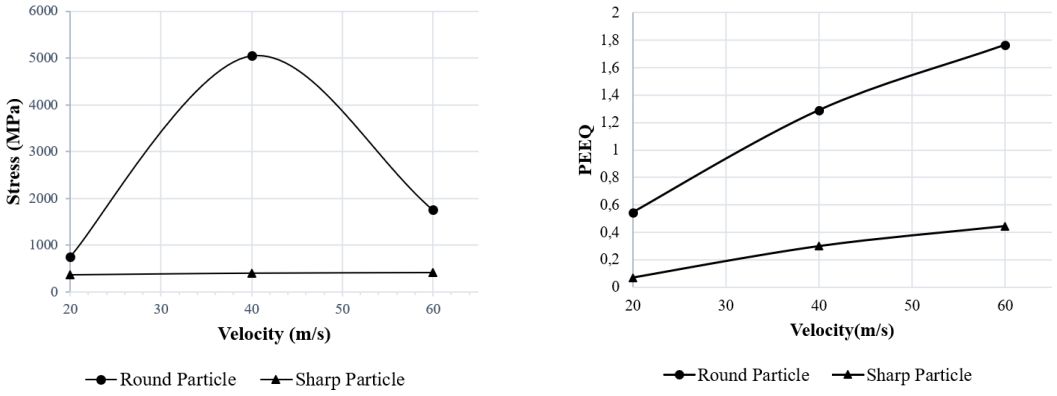

(a) (b)

Figure 4. (a) Stress versus velocity; (b) PEEQ versus Velocity

When analyzing figure 4 and figure 5, it was possible to observe that the increase in speed significantly influences the materials involved in the impact. It is noted that for the contact between the sphere and the flat counterpart, the increase in velocity generates great deformation in the projectile, so that the increase in the impact velocity makes the geometry of the projectile more elliptical, generation maximum equivalent stresses of 753 MPa to a speed of 20 m/s, 5049 MPa at 40 m/s and 1753 MPa at 60 m/s, and the flat counterpart has no deformation in the range of analyzed speed. The impact of sharp projectile generates lower stresses when compared to the sphere projectile, but causes relevant impacts to the flat counterpart, generating maximum equivalent stresses of 362MPa for a speed of 20 m/s, 395 MPa at 40 m/s and 409 MPa at 60 m/s, so that with the increase in the impact speed, there is an increase in the stress and deformation of the two materials, with the projectile losing mass and the flat counterpart generation significant plastic deformations.

The equivalent plastic strain (PEEQ) is a scalar variable that is used to represent the material's inelastic deformation. If this variable is greater than zero, the material has yielded, figure 4(b) shows that both the spherical particle and the pointed particle generate greater plastic.

Thus, it is possible to conclude that the impact of the sharp projectile is more critical for the flat counterpart and the impact of the spherical projectile generates deformation for the sphere itself, with little influence on the flat counterpart.

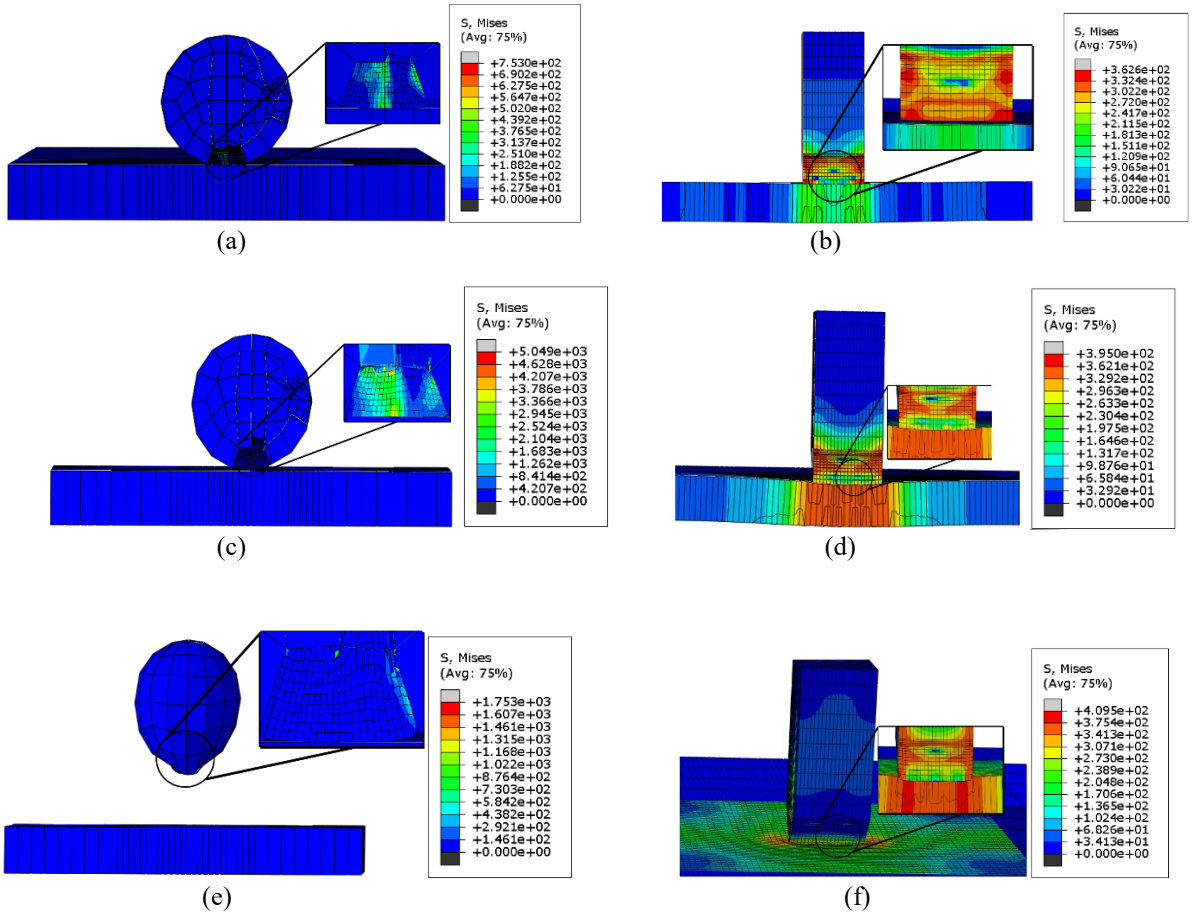

Figure 5. Result of impact between deformable particles: (a) Sphere at 20 m/s- Flat counterpart; (b) Sharp at 20 m/s – Flat counterpart; (c) Sphere at 40 m/s- Flat counterpart; (d) Sharp at 40 m/s – Flat counterpart; (e) Sphere at 60 m/s- Flat counterpart; (d) Sharp at 60 m/s – Flat counterpart.

4 Conclusion

The comparison between analytical and numerical solutions shows us an excellent agreement of the results obtained when analyzing in a specific period of contact time. From the numerical simulation created, it was possible to analyze the contact pressure distribution and to evaluate the indentation depth at the center of the contact zone. For validation of the impact simulation, the analyzes were carried out within the elastic regime at small strains and compared to the Hertz's equations. Sufficient low impact velocities have been used, so that it most of the energy was dissipated as deformations. The average difference between the results was less than 10%, this deviation can be justified by the coarse mesh used in this study. This aspect of the model will be a subject of a future work.

From the impact analysis, using CDP model for the brittle particles and the Johnson-Cook model for the flat steel counterpart, it was possible to observe that an increase in velocity leads to severe deformations on the flat surface. The sharp projectile shows significantly more stress to the flat counterpart while displaying much less strain on its own surface. The opposite behavior is observed on sphere-to-flat configuration where most of the deformation is seen on the projectile while the counterpart shows minute stresses.

In a following work, the analysis of cyclical impact, the damage evolution and the fracture phenomena will be addressed.

References

[1] Pereira O.A.G, Araujo S.G.A, Doca T. Analysis of erosive damage in flail mower protective frame FLV 225. 25th International Mechanical Engineering Congress – DOI: 10.26678/ABCM.COBEM 2019.COB2019-0890.
[2] Finnie I; WOLAK, J.; KABIL, Y. Erosion of metals by solid particles, ASTM J. Mater., 2 (1967).
[3] Goodman E.R. Introduction to Rock Mechanics. WILEY, Canada, 2nd Edition. (1989).
[4] Johnson, K.L. Contact mechanics, Cambridge University Press (1985).
[5] Hertz, H.R. Ueber die Beruehrung elastischer Koerper (On Contact Between Elastic Bodies), 1882.
[6] Doca, T. PRODEM Seminar on Computational Contact Mechanics. 2010.
[7] Cattaneo, C. Sul contatto di due corpi elastici: distribuzione locale degli sforzi. Rend. Accad. Naz. Lincei, v. 27, n. 6, p. 342–348 (1938).
[8] Mindlin, R.D. Compliance of elastic bodies in contact. Journal of applied mechanics, v. 16, p. 159–268 (1949).
[9] Abaqus Theory Manual. Abaqus User's Man. Version 6.8, n.d.
[10] Kiran, S. Finite element simulations of ballistic impact on metal and composite plates, 2004.
[11] Johnson G. R. and Cook W. H. : A constitutive model and data for metals subjected to large strains, high strain rates and high temperature.
[12] Liang R. and Khan A.S : A critical review of experimental result and constitutive models for BCC and FCC metal over a wide range of strain rates and temperature.
[13] Wang, J., Yin, Y., Luo, C.: Johnson–Holmquist-II(JH-2) constitutive model for rock materials: parameter determination and application in tunnel smooth blasting. Appl. Sci. 8, 1675 (2018)
[14] Lubliner, J. Oliver, J. Oller, S. Onate, E. A plastic-damaged model for concrete. International Journal of Solids and Structures.Great Britain,v. 25, n. 3, p. 299-326, 1989.
[15] Lee, Jeeho. FENVES, Gregory L. Plastic-damaged model for cyclic loading of concrete structures. Journal of Engineering Mechanics. 1998.
[16] Simulia. Abaqus analysis user's manual. USA, 2012.
[17] Johnson, G. R., COOK, W.H. – Fracture characteristics of three metals subjected to various strain rates, temperatures and pressures – Engineering Fracture Mechanics, vol 21, No. 1, 1985.
[18] Jaspers, S. P. F. C., & Dautzenberg, J. H. (2002). Material Behavior in Conditions Similar to Metal Cutting: Flow Stress in the Primary Shear Zone. J. Mater. Process. Technol., Vol. 122, pp. 322–330.
[19] Mojtaba Labibzadeh, Mojtaba Zakeri, Abdol Adel Shoaib, (2017) "A new method for CDP input parameter identification of the ABAQUS software guaranteeing uniqueness and precision", International Journal of Structural Integrity, Vol. 8 Issue: 2, pp.264-284.
[20] JOHNSON, G. R., COOK, W. H. A constitutive model and data for metals subjected to large strains, high strain rates and high temperatures. Proc. 7th Int. Symp. on BuNistics, pp. 541547. The Hague, The Netherlands. April, 1983.